We are IntechOpen, the world's leading publisher of Open Access books Built by scientists, for scientists

6,900
Open access books available

185,000
International authors and editors

200M
Downloads

Our authors are among the

154
Countries delivered to

TOP 1%
most cited scientists

12.2%
Contributors from top 500 universities

WEB OF SCIENCE™

Selection of our books indexed in the Book Citation Index in Web of Science™ Core Collection (BKCI)

Interested in publishing with us?
Contact book.department@intechopen.com

Numbers displayed above are based on latest data collected.
For more information visit www.intechopen.com

8

Continental Erosion/Weathering Changes in Central Asia Recorded in the Holocene Sediment from Lake Hovsgol, Northwest Mongolia, by Synchrotron μ-XRF Mapping Analyses

Nagayoshi Katsuta[1], Takuma Murakami[2,3], Yuko Wada[2], Masao Takano[2], Masayuki Kunugi[4] and Takayoshi Kawai[2,5]
[1]*Faculty of Education, Gifu University*
[2]*Graduate School of Environmental Studies, Nagoya University*
[3]*Low Level Radioactivity Laboratory, Kanazawa University*
[4]*Environment Safety Center, Tokyo University of Science*
[5]*Association of International Research Initiatives for Environmental Studies*
Japan

1. Introduction

Lake Hovsgol (Fig. 1) is located in the southernmost part of the Baikal rift valley basins and occupies the second largest basin next to Lake Baikal. The lake lies 1645 m above sea level, and its surface area is 2,760 km^2 (136 km long, 20~40 km wide). It has a water volume of 380.7 km^3 and a maximum depth of 262.4 m (Goulden et al., 2006). The lake is surrounded by three types of vegetation regions: taiga-forest, steppe, and steppe-forest. The annual mean temperature is below zero (above zero during May to September), and the precipitation is 300~500 mm per year, most of which falls from April to October (Namkhaijantsan, 2006). The lake water contains Ca^{2+} at 797 μM. Its alkalinity is 2.60 (mEq/L), and it has a pH of 8.1 (Hayakawa et al., 2003). Geophysical observations reveal that Hovsgol's sediment is several kilometers thick (Fedotov et al., 2006), which suggests that the sedimentary sequences may document a long-term history of environmental changes in arid central Asia.

Recent studies on Lake Hovsgol cores indicate that the sediment chemistry records are important sources of information to understand environmental variations in the region and related climate changes. Oscillations in the climate proxy data acquired by stack of elements hosted in the carbonates and organic matter have been found to coincide with abrupt climate shifts in the Holocene and the last glacial/Holocene transition observed in the North Atlantic region (Fedotov et al., 2004a). Periodic variations in the 21 chemical elements in the bulk-sediment suggested that moisture change in central Asia occurred on glacial-interglacial scales, as well as with a period of ~8.7 kyr, through the last glacial/Holocene (Murakami et al., 2010). Phedorin et al. (2008) analyzed the past 1 Myr geochemical records

of sediments from the two great Asian lakes (Hovsgol for Ti/Ca and Br; Baikal for diatoms and Br) with a synchrotron radiation (SR) induced μ-XRF line-scanning technique, and then found a 300-500 kyr long cycle, possibly associated with Earth's orbital eccentricity. Moreover, Phedorin et al. (2008) suggested that the variations with periods of 300-500 kyr influenced the evolution of terrestrial ecosystem.

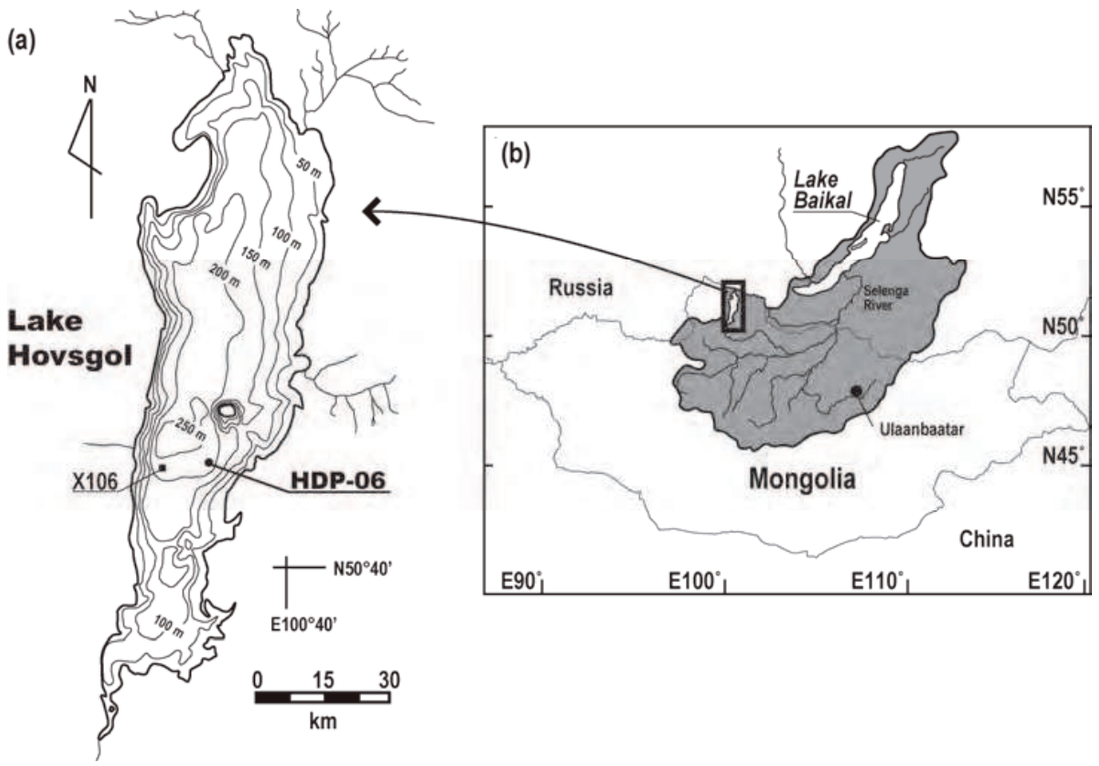

Fig. 1. Maps of (a) Lake Hovsgol in (b) northern Mongolia. (a) Bathymetric map of the lake showing drill sites for cores X106 and HDP-06. HDP-06 was used for analyses in the present study. The gray shading and lines in (b) indicate the Lake Baikal catchment area and the borders of China, Mongolia, and Russia, respectively.

In the present study, we investigated the distributions and their origins of 11 major and trace elements in the Holocene section of Hovsgol's sediment using the SR μ-XRF mappings. With respect to the Hovsgol's sediment, the two-dimensional distribution of the elements has not been studied until now. A visualization of distribution of the elements enables us to recognize detailed sedimentary or geochemical structures such as laminations, local elementally enriched grains and layers, and so on (Katsuta et al., 2007). Moreover, it makes possible to distinguish between primary structures and secondary structures deposited in the sediment. As a result of this study, we discovered an alternation of terrigenous and biological elements in the Hovsgol Holocene sections. In this chapter, we first describe methods for capturing the SR μ-XRF data of the sediment surfaces. After investigating distributions and features of the detected 11 elements, we assess the sources and natures of each element. We discuss the paleoenvironmental implications for the observed alternated pattern in the sedimentation, together with a record of the detritus input into Lake Hovsgol (Murakami et al. 2010).

2. Materials and analytical methods

2.1 Core HDP-06

In the present study, we used core HDP-06 which was collected at the base of the southeast slope of Lake Hovsgol, in northwest Mongolia (Fig. 1). The HDP-06 core drilling took place in March 2006 at 50°54′25″ N, 100°27′03″ E at a water depth of 235.5 m using an improvised push-coring type technology (Hovsgol Drilling Project Members, 2009). Core HDP-06 was about 26 m long and the sediment recovery was on the order of 80%. In the present study, we analyzed the upper section (about 18 cm) of HDP-06 core 1-1 (about 140 cm), which was undisturbed and fully recovered. The lithologic observation revealed that the core 1-1 bears sedimentary layers distinctive of Hovsgol's sediment, which is composed of diatomaceous clayey ooze in the Holocene section and calcareous clayey silt to silty clay in the last glacial section (Prokopenko et al., 2005).

2.2 Sample preparations

In order to acquire two-dimensional XRF images of the sediment surface by the SR μ-XRF techniques, we prepared thin sections of the resin-embedded samples. Subsamplings from an open core surface were carried out using aluminum U-channels (Fig. 2). After carefully retrieving the sediment slab from the U-channel, the slabs were impregnated with epoxy resin following the procedure of Tiljander et al. (2002). The U-channels were produced from a 0.2-mm-thick aluminum sheet using a sheet bender (Fig. 2a), which we produced ourselves.

A resin-embedded sediment block was shaped to a thickness of 0.3 mm for SR μ-XRF mapping. This was done to reduce the X-ray scattering from the inside of the sample. First, a pair of sediment slabs (Fig. 3a) was separated with a band saw because several sediment slabs were embedded together with the epoxy resin. Each sediment slab was cut into three pieces to produce approximately 5 cm × 5 cm samples at an angle of 45° to the bedding plane (Fig. 3b), in order to maintain the vertical continuity of the sediment. One face of each sample was polished and glued to a glass slide. After polishing the other face to achieve a thickness of about 0.3 mm, the thin section sample (Figs. 3c and d) was removed from the glass slide using a solvent.

2.3 SR μ-XRF mapping

The SR experiment was carried out at undulator beamline 37XU of SPring-8, Hyogo, Japan (Fig. 4a; Terada et al., 2004). A Si (111) double-crystal monochromator was used to acquire the incident X-ray beams at 37 keV. The X-ray beam size was adjusted using an XY slit and was 1 mm (V) × 0.5 mm (H). A thin-section sample was fixed on an acrylic holder (Fig. 3c). The sample holder was set on the X-Y computer-controlled step stage, which was rotated by 10^{o} in the rectangular direction of the incident beam toward the detector (Fig. 3d). The stage had step sizes of 1 mm (V) and 0.5 mm (H). The XRF spectra from the sample were measured using a Ge solid-state detector coupled with a multichannel pulse-height analyzer (Fig. 4a). The measurement time was 25 s per step.

In Hovsgol's sediment, fluorescence X-rays of the 11 elements (Ti, Mn, Fe, Cu, Zn, As, Br, Rb, Zr, and Nb) were successfully detected (Figs. 4b and c). Based on the obtained XRF spectra, we determined the distribution map and profile of each element (Fig. 5). The XRF spectra were collected at each position on a sample. At each position, we computed the integrated numbers of X-ray photons with energy near each Ka_1 line (energy window within $Ka_1 \pm 0.10$ keV), and consequently produced XRF maps of the 11 elements. Moreover, the XRF profiles were acquired by averaging three vertical lines of the XRF maps, which were appropriately selected.

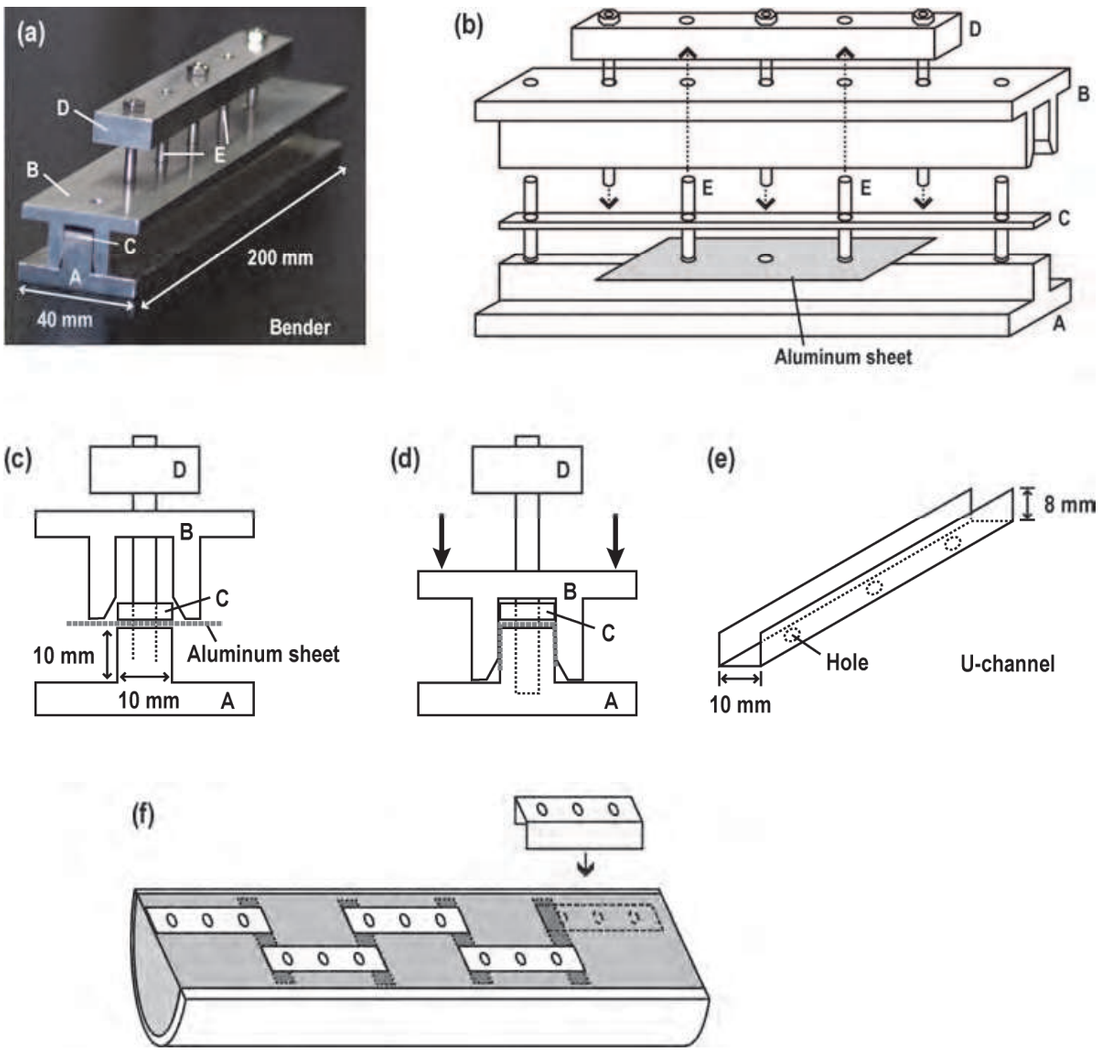

Fig. 2. Tools for subsampling open core surface. (a–d) Photograph and schematic sketches showing a sheet bender made of aluminum. (e) Schematic sketch showing an aluminum U-channel. An aluminum sheet (0.2 mm thick) was first cut into 120 mm × 36 mm rectangular pieces with a shearing machine, which in turn was set on a male die A with rods E (b). After pressing a female punch B and plank with rods D downward (c and d), the U-channel (e) was produced. Finally, the sample number and direction were inscribed onto the back of the U-channel using a scriber. The produced aluminum U-channels are pressed into halved cores, with adjacent U-channels overlapping each other as shown in (f). The sediment-filled U-channels were carefully extruded from the split cores using a metal spatula. The hole positions of an aluminum sheet (b) coincide with the positions of holes in B-D and rods E, and the holes have slightly large diameter compared with the rods. The insertion of the three rods in D and E into the corresponding holes in aluminum sheet (b) prevented the movement of the sheet during bending and simultaneously allowed the sheet to be bent at a right angle. Rods E were screwed into a male punch A like D, thereby allowing easy removal of the produced U-channel from the punch. The holes in U-channel (e) aided fluid flow in the later impregnation stage.

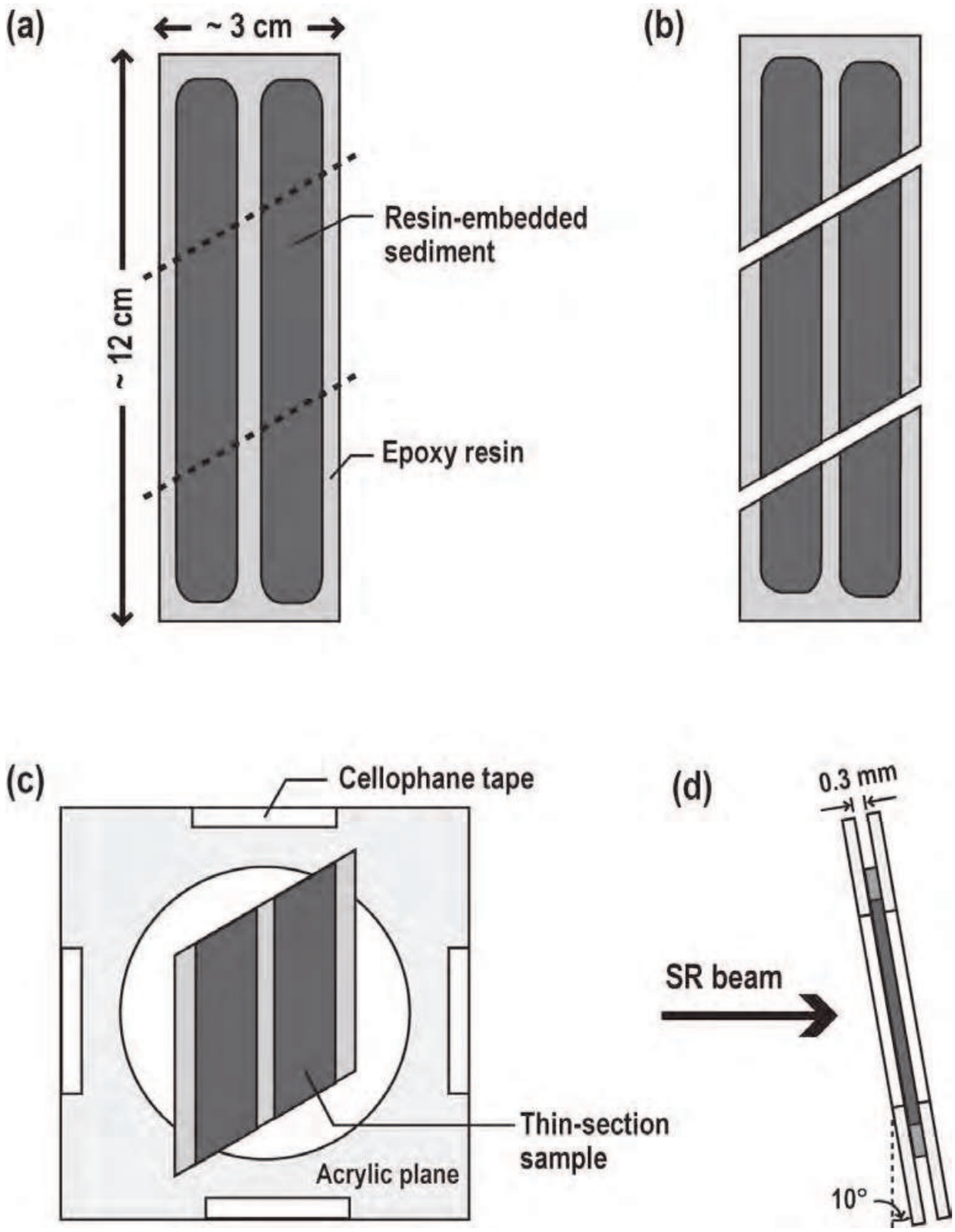

Fig. 3. Schematic diagrams of resin-embedded sediment sample and its experimental setup. (d) is indicated by red rectangle in Fig. 4a.

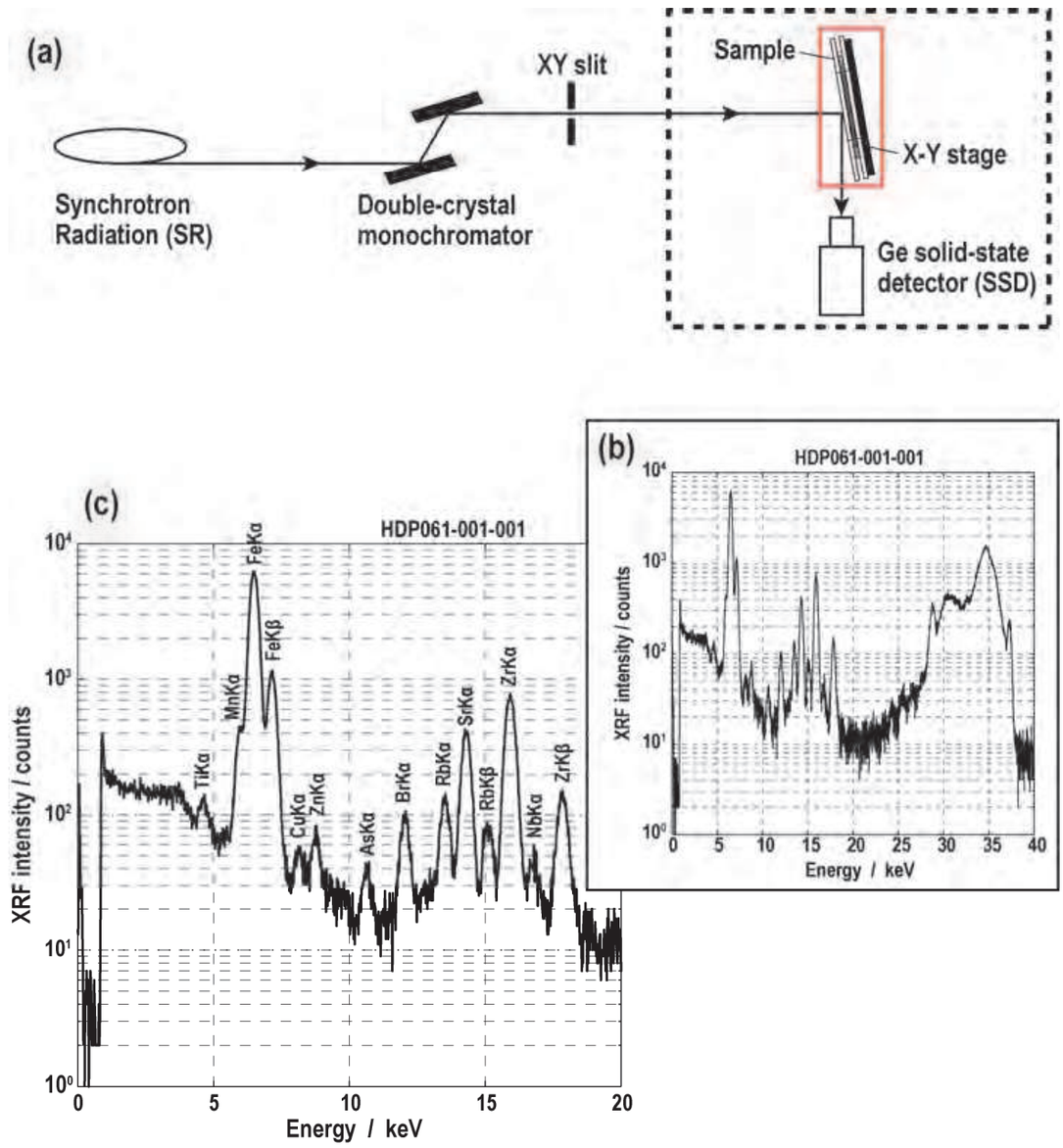

Fig. 4. (a) Schematic sketch showing experimental setup for SR μ-XRF mapping at BL37XU of SPring-8 and XRF spectra in ranges of (b) 0–40 keV and (c) 0–20 keV for upper section of HDP-06 core 1-1 from Lake Hovsgol. Sample of red rectangle in (a) corresponds to Fig. 3d.

3. Results and discussions

3.1 Distribution of elements in Lake Hovsgol sediment

Successive maps and profiles of the 11 elements in the upper section of HDP-06 core 1-1 are shown in Fig. 5. From a visual inspection of the distribution and features, the 11 elements were classified into three assemblages–group 1: Ti, Fe, Cu, Zn, As, Rb, Sr, Zr, and Nb; group 2: Br; and group 3: Mn, Fe, and As. Their distributions in the sediment are characterized as follows:

1. Groups 1 and 2 consist of several centimeter-scale layers that alternate with each other (Figs. 5a and c–k).
2. The manganese of group 3 is irregularly distributed over the entire section, occurring in thin layers and spots (Fig. 5b).
3. A portion of the arsenic from group 3 occurs in thin layers, together with Fe (Figs. 5c and f).

Based on the distributions and assemblages of the elements, group 1 is recognized to be elements composed of rock-forming minerals in the bedrock of the Hovsgol basin (Murakami et al., 2010). The group 1 is therefore terrigenous elements, which were supplied from the drainage basin by erosion and weathering processes. Bromine belonging to group 2 is a biophilic element whose abundance variation in the sediment reflects bioproduction in the lake (Phedorin et al., 2008). In Lake Hovsgol, the record of Br as alternative to diatom and bioSi, especially in the bottom sediment below 5.74 m (Fedotov et al., 2004b), is an important source of information to estimate biogenic production of the lake because the diatom frustules may be dissolved in the sediment high-pH pore water resulting from the presence of carbonates.

Manganese, Fe, and As of group 3 are elements sensitive to redox condition in the sediment. Existences of these three elements were indentified also in core X106 (Murakami et al. 2010). According to the study, the Mn in the core showed irregular distributions from the last glacial/Holocene transition to the Holocene section. The XRD analyses didn't indicate peaks of minerals containing Mn, thereby suggesting that the Mn in the sediment exists in an amorphous state. On the other hand, the coexistence of Fe and As identified in this study (red arrows in Figs. 5c and f) were identified in the last glacial/Holocene transition section of core X106. Because the section contains pyrite and dolomite as well as arsenic, Murakami et al. (2010) suggested the presence of sulfate-reducing bacteria.

These three elements of group 3 may have responded to redox changes and have subsequently migrated during the diagenetic process in the sediment. We therefore investigate paleoenvironmental implications for variations in the group 1 terrigenous elements and group 2 Br records of core HDP-06, as discussed below.

3.2 Continental erosion/weathering changes in central Asia during the Holocene period

Comparison of the terrigenous elements of group 1 (Ti, Fe, Cu, Zn, As, Rb, Sr, Zr, and Nb) with the Br of group 2 in the HDP-06 core 1-1 indicates a strong counterphase in the Holocene section (Fig. 5). At the present stage, the age of the section has not yet been determined. However, as shown in Figs. 6b and c, the content variation of Ti in the HDP-06 sediment is well correlative with that of dated X106 core (Murakami et al., 2010). Accordingly, by a correlation between these two profiles, we discuss hereafter nature of the temporal content variations of Ti and Br in HDP-06 core, together with paleoproxy records of X106 core.

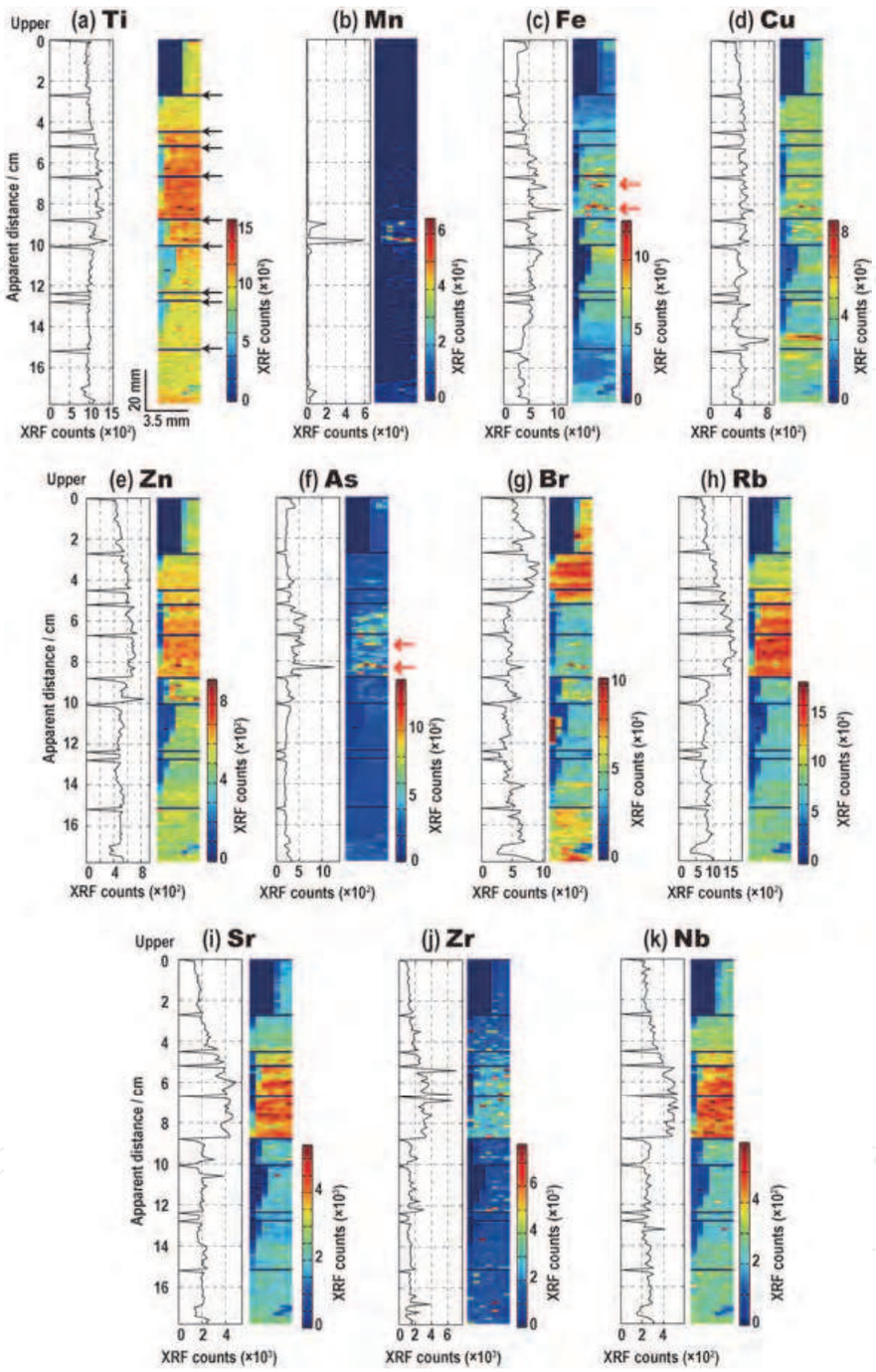

Fig. 5. Successive maps and profiles of major and trace elements in upper section of HDP-06 core 1-1: (a) Ti, (b) Mn, (c) Fe, (d) Cu, (e) Zn, (f) As, (g) Br, (h) Rb, (i) Sr, (j) Zr, and (k) Nb. The black arrows in (a) show the boundaries between the neighboring measurement areas, which were overlapped by approximately several millimeters. The vertical distance of each element profile hence represents the apparent core depth. The red arrows in (e) and (f) show the coexistence of Fe and As. The low XRF counts seen on the left side of each map were caused by the epoxy resin.

Figure 6 shows successive profiles for sediment chemistry of Lake Hovsgol, atmospheric CO_2 (Indermühle et al. 1999), and general circulation model (GCM)-predicted climatic parameters in central Asia (Bush, 2005). The second principal component (PC-2) score (Fig. 6d) was obtained by principal component analysis of 21 chemical components in bulk-sediment of X106 core by the ICP-MS (inductively coupled plasma mass spectrometry) analyses (Murakami et al., 2010). The variability of the PC-2 score was controlled by chemical elements from detrital materials, thereby indicating erosion/weathering intensity in the Hovsgol drainage basin. Temporal variations of annual mean temperature and precipitation minus evaporation (PME) in central Asia (Figs. 6e and f) are GCM outputs of simulation accounting to the combined effect of orbital and CO_2/H_2O (Fig. 6g) forcing.

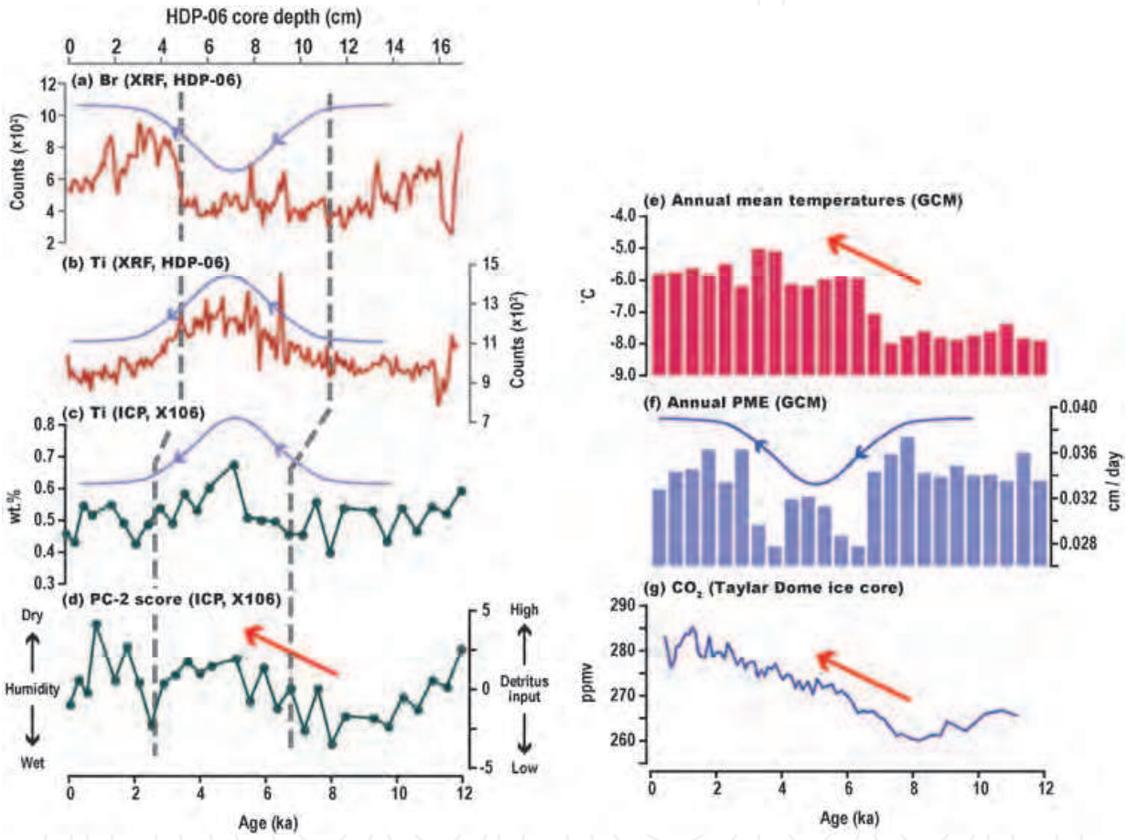

Fig. 6. Comparison of (a)-(d) paleoenvironmental proxy records from Lake Hovsgol, (e)-(f) GCM-simulated selected climatic parameters over central Asia (Bush, 2005), and (g) atmospheric CO_2 concentration record from Antarctica ice core at Talyor Dome (Indermühle et al., 1999) over the Holocene interval. (a) Br and (b) Ti profiles in Lake Hovsgol sediment of HDP-06 core 1-1 are captured by the SR μ-XRF analysis. (c) Ti and (d) PC-2 score in Lake Hovsgol core X106 are from Murakami et al. (2010). PME in (f) stands for precipitation minus evaporation. Arrows with curved or straight lines denoted in each plot emphasize significant environmental/climatic trend. The horizontal scale in (a)-(b) and that in (c)-(g) are shown by the core depth in the upper axis and by the age in lower axis, respectively. Vertical gray dashed lines in (a)-(d) indicates a visual correlation of Ti in cores between HDP-06 and X106.

The variations of Ti and Br contents in core HDP-06 are similar to that of PME over the Holocene period (Figs. 6a, b, and f). The relationship between Ti and PME shows an inverse correlation, whereas the relationship between Br and PME shows a positive correlation. In the mid-Holocene, the Ti intensity peaks at low PME, and the Br content increases in the early- and late-Holocene when the PME rises. On the other hand, the PC-2 score in core X106 (Fig. 6d), together with annual mean temperature in central Asia (Fig. 6e) and atmospheric CO_2 concentration (Fig. 6f), shows a gradual increase from about 8.0 ka to the present day.

These two-type variations observed in cores HDP-06 and X106 are considered to have resulted from changes in erosion/weathering intensity of central Asia (Asian continental interior) with moisture changes.

Evidences and suggestions supporting our hypothesis are provided by studies on the sediment from Lake Hovsgol. Prokopenko et al. (2007) showed that the early Holocene diatom/biogenic silica (bioSi) peaks correlated with the humidity maximum (Fig. 6f) reconstructed by the pollen fossil analyses and from predictions of GCMs (Bush, 2005). Based on these observations, Prokopenko et al. (2007) regarded that the early Holocene increase of diatom abundance in Lake Hovsgol was caused by increased nutrient supply with high precipitation and surface runoff. The early Holocene diatom/bioSi peaks correspond to the increased Br contents in core HDP-06 (Fig. 6a). Murakami et al. (2010) observed that low PC-2 detrital input occurred during the early Holocene (Fig. 4d). To explain the early Holocene decease of erosion/weathering intensity in the drainage basin with high humidity, Murakami et al. (2010) proposed that the detritus supply to Lake Hovsgol may have been controlled by the amount of vegetation cover: (1) vegetation cover in the catchment increased with high precipitation; (2) as a result, the nutrient supply to the lake enhanced, which in turn resulted in high productivity in the lake; (3) simultaneously, declined erosion through the drainage basin resulted in a reduced sediment supply into the lake.

The interpretation for the early Holocene detritus input by Murakami et al. (2010) can apply to the gradual increase from about 8.0 ka observed in the PC-2 score (Fig. 6d), the regional annual mean temperature (Fig. 6e), and atmospheric CO_2 concentration (Fig. 6g): (1) the annual mean temperature increases with the rise in atmospheric CO_2; (2) because of the exponential increase of the saturation vapor pressure with air temperature, the moisture decreases; (3) the resultant aridity of the continental interior has intensified the erosion/weathering processes.

4. Conclusions

We measured nondestructively 11 major and traces elements in the Holocene sediment of core HDP-06 core from Lake Hovsgol, using SR μ-XRF mapping techniques. A visual inspection of the acquired XRF images revealed that the 11 elements were classified into the three assemblages–group 1: Ti, Fe, Cu, Zn, As, Rb, Sr, Zr, and Nb, composed of rock-forming minerals; group 2: Br, recognized as a biophilic trace elements; and group 3: Mn, Fe, and As, sensitive to redox condition in the sediment.

Temporal variations in the first two groups, based on the age of core X106, are in phase with GCM-simulated PME in central Asia. This trend is remarkably different from the PC-2 score of core X106 indicating detritus input into the lake. The PC-2 score, together with atmospheric CO_2 and the regional annual mean temperature, shows a gradual increase from

early Holocene to the present day. These two-type variations suggest that the continental erosion/weathering in central Asia occurred on two different processes and time-scales.

5. Acknowledgement

The authors are very grateful to the staff of Technical Center of Nagoya University. K. Suzuki provided helpful support in designing a sheet bender. S. Yogo made many helpful suggestions on sample preparation. A part of μ-XRF analysis was performed with the approval of SPring-8 (Proposal No. 2006B1091 and 2007A1563). We also thank to Y. Terada for μ-XRF mappings using synchrotron radiation. We are grateful to the HDP members for subsampling from the HDP-06 core. This study was supported by the Sumitomo Foundation grant No.103359; the Saijiro Endo Memorial Foundation; awards from Dynamics of the Sun-Earth-Life Interactive System, No. G-4 at Nagoya Univ., and Environmental Monitoring and Prediction of Long- and Short-Term Dynamics of Pan-Japan Sea Area, No. E-07 at Kanazawa Univ., of the 21st Century COE Program of the Ministry of Education, Culture, Sports, Science and Technology, Japan.

6. References

Bush, A. B. G. (2005). CO_2/H_2O and orbitally driven climate variability over central Asia through the Holocene. *Quaternary International,* Vol. 136, No. 1, pp. 15-23. ISSN 1040-6182

Fedotov, A. P., Chebykin, E. P., Semenov, M. Y., Vorobyova, S. S., Osipov, E. Y., Golobokova, L. P., Pogodaeva, T. V., Zheleznyakova, T. O., Grachev, M. A., Tomurhuu, D., Oyunchimeg, T., Narantsetseg, T., Tomurtogoo, O., Dolgikh, P. T., Arsenyuk, M. I. & De Batist, M. (2004a). Changes in the volume and salinity of Lake Khubsugul (Mongolia) in response to global climate changes in the upper Pleistocene and the Holocene. Palaeogeography, Palaeoclimatology, Palaeoecology, Vol. 209 Nos. 1-4, pp. 245–257, ISSN 0031-0182

Fedotov, A., Kazansky, A. Y., Tomurhuu, D., Matasova, G., Ziborova, G., Zheleznyakova, T., Vorobyova, S., Phedorin, M., Goldberg, E., Oyunchimeg, T., Narantsetseg, T., Vologina, E., Yuldashev, A., Kalugin, I., Tomurtogoo, O. & Grachev, M. (2004b). A 1-Myr record of paleoclimates from Lake Khubsugul, Mongolia. *EOS, Transactions, American Geophysical Union,* Vol. 85, No. 40, pp. 387, 390, ISSN 0096-3941

Fedotov, A., San'Kov, V., De Batist, M., Kazansky, A., Parfeevets, A., Miroshnitchenko, A. & Pouls, T. (2006). Chronology of the Baikal rift system. *EOS, Transactions, American Geophysical Union,* Vol. 87, No. 25, pp. 246, 250, ISSN 0096-3941

Goulden, C. E., Tumurtogoo, O., Karabanov, E. & Mongontsetseg, A. (2006). The geological history and geography of Lake Hövsgöl, In: *The Geology, Biodiversity and Ecology of Lake Hövsgöl (Mongolia),* Goulden, C. E., Sitnikova, T., Gelhaus, J. & Boldgiv, B., pp. 1–19, Leiden, The Netherlands, ISBN 9057821621

Hayakawa, K., Sekino, T., Yoshioka, T., Maruo, M. & Kumagai, M. (2003). Dissolved organic carbon and fluorescence in Lake Hovsgol: factors reducing humic content of the lake water. Limnology, Vol. 4, No. 1, pp. 25–33, ISSN 1439-8621

Hovsgol Drilling Project Members (2009). Sedimentary record from Lake Hovsgol, NW Mongolia: Results from the HDP-04 and HDP-06 drill cores. *Quaternary International,* Vol. 205, No. 1-2, pp. 21–37, ISSN 1040-6182

Indermühle, A., Stocker, T. F., Joos, F., Fischer, H., Smith, H. J., Wahlen, M., Deck, B., Mastroianni, D., Tschumi, J., Blunier, T., Meyer, R. & Stauffer, B. (1999). Holocene carbon-cycle dynamics based on CO_2 trapped in ice at Taylor Dome, Antarctica. Nature, Vol. 398, No. 6723, pp. 121-126, ISSN 0028-0836

Katsuta, N., Takano, M., Kawakami, S., Togami, S., Fukusawa, H., Kumazawa, M. & Yasuda, Y. (2007). Advanced micro-XRF method to separate sedimentary rhythms and event layers in sediments: its application to lacustrine sediment from Lake Suigetsu, Japan. *Journal of Paleolimnology,* Vol. 37, No. 2, pp. 259–271, ISSN 0921-2728

Murakami, T., Katsuta, N., Yamamoto, K., Takamatsu, N., Takano, M., Oda, T., Matsumoto, G. I., Horiuchi, K. & Kawai, T. (2010). A 27-kyr record of environmental change in central Asia inferred from the sediment record of Lake Hovsgol, northwest Mongolia. *Journal of Paleolimnology,* Vol. 43, No. 2, pp. 369–383, ISSN 0921-2728

Namkhaijantsan, G. (2006). Climate of the Hövsgöl Lake region, In: *The Geology, Biodiversity and Ecology of Lake Hövsgöl (Mongolia),* Goulden, C. E., Sitnikova, T., Gelhaus, J. & Boldgiv, B., pp. 63–76, Leiden, The Netherlands, ISBN 9057821621

Phedorin, M. A., Fedotov, A. P., Vorobieva, S. S. & Ziborova, G. A. (2008). Signature of long supercycles in the Pleistoncene history of Asian limic systems. *Journal of Paleolimnology,* Vol. 40, No. 1, pp. 445–452, ISSN 0921-2728

Prokopenko, A.A., Khursevich, G. K., Bezrukova, E. V., Kuzmin, M. I., Boes, X., Williams, D. F., Fedenya, S. A., Kulagina, N. V., Letunova, P. P. & Abzaeva, A. A. (2007). Paleoenvrionmental proxy records from Lake Hovsgol, Mongolia, and a synthesis of Holocene climate change in the Lake Baikal watershed. *Quaternary Research,* Vol. 68, No. 1, pp. 2-17, ISSN 0033-5894

Prokopenko, A. A., Kuzmin, M. I., Williams, D. F., Gelety, V. F., Kalmychkov, G. V., Gvozdkov, A. N. & Solotchin, P. A. (2005). Baisn-wide sedimentation changes and deglacial lake-level rise in the Hovsgol basin, NW Mongolia. *Quaternary International,* Vol. 136, No. 1, pp. 59–69, ISSN 1040-6182

Terada, Y., Goto, S., Takimoto, N., Takeshita, K., Yamazaki, H., Shimizu, Y., Takahashi, S., Ohashi, H., Furukawa, Y., Matsushita, T., Ohata, T., Ishizawa, Y., Uruga, T., Kitamura, H., Ishikawa, T. & Hayakawa, S. (2004). Construction and commissioning of BL37XU at SPring-8. *AIP Conference Proceedings,* Vol. 705, pp. 376-379, ISSN 0094-243X

Tiljander, M., Ojala, A., Saarinen, T. & Snowball, I. (2002). Documentation of the physical properties of annually laminated (varved) sediments at a sub-annual to decadal resolution for environmental interpretation. *Quaternary International,* Vol. 88, No. 1, pp. 5–12, ISSN 1040-6182

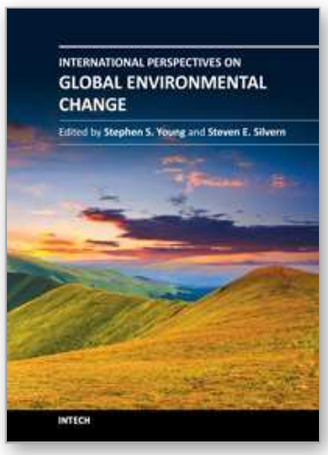

International Perspectives on Global Environmental Change

Edited by Dr. Stephen Young

ISBN 978-953-307-815-1
Hard cover, 488 pages
Publisher InTech
Published online 03, February, 2012
Published in print edition February, 2012

Environmental change is increasingly considered a critical topic for researchers across multiple disciplines, as well as policy makers throughout the world. Mounting evidence shows that environments in every part of the globe are undergoing tremendous human-induced change. Population growth, urbanization and the expansion of the global economy are putting increasing pressure on ecosystems around the planet. To understand the causes and consequences of environmental change, the contributors to this book employ spatial and non-spatial data, diverse theoretical perspectives and cutting edge research tools such as GIS, remote sensing and other relevant technologies. International Perspectives on Global Environmental Change brings together research from around the world to explore the complexities of contemporary, and historical environmental change. As an InTech open source publication current and cutting edge research methodologies and research results are quickly published for the academic policy-making communities. Dimensions of environmental change explored in this volume include: Climate change Historical environmental change Biological responses to environmental change Land use and land cover change Policy and management for environmental change

How to reference

In order to correctly reference this scholarly work, feel free to copy and paste the following:

Nagayoshi Katsuta, Takuma Murakami, Yuko Wada, Masao Takano, Masayuki Kunugi and Takayoshi Kawai (2012). Continental Erosion/Weathering Changes in Central Asia Recorded in the Holocene Sediment from Lake Hovsgol, Northwest Mongolia, by Synchrotron μ-XRF Mapping Analyses, International Perspectives on Global Environmental Change, Dr. Stephen Young (Ed.), ISBN: 978-953-307-815-1, InTech, Available from: http://www.intechopen.com/books/international-perspectives-on-global-environmental-change/continental-erosion-weathering-changes-in-central-asia-recorded-in-the-holocene-sediment-from-lake-h

INTECH
open science | open minds

InTech Europe
University Campus STeP Ri
Slavka Krautzeka 83/A
51000 Rijeka, Croatia
Phone: +385 (51) 770 447
Fax: +385 (51) 686 166
www.intechopen.com

InTech China
Unit 405, Office Block, Hotel Equatorial Shanghai
No.65, Yan An Road (West), Shanghai, 200040, China
中国上海市延安西路65号上海国际贵都大饭店办公楼405单元
Phone: +86-21-62489820
Fax: +86-21-62489821

© 2012 The Author(s). Licensee IntechOpen. This is an open access article distributed under the terms of the Creative Commons Attribution 3.0 License, which permits unrestricted use, distribution, and reproduction in any medium, provided the original work is properly cited.

IntechOpen

IntechOpen